Available online at www.sciencedirect.com

ScienceDirect

Journal of Non-Crystalline Solids 354 (2008) 2598–2602

JOURNAL OF NON-CRYSTALLINE SOLIDS

www.elsevier.com/locate/jnoncrysol

Comparison of three un-cooled micro-bolometers configurations based on amorphous silicon–germanium thin films deposited by plasma

M. Moreno, A. Kosarev *, A. Torres, R. Ambrosio

National Institute for Astrophysics, Optics and Electronics, Puebla, Mexico, P.O. Box 51 and 216, Puebla, Z.P. 7200, Puebla, Mexico

Available online 17 March 2008

Abstract

We present a comparative study of three configurations of un-cooled micro-bolometers based on amorphous silicon–germanium thin films deposited by plasma at low temperature and compatible with the IC technology. The temperature dependence of conductivity $\sigma(T)$, current–voltage characteristics $I(U)$ and current noise spectral density (NSD) have been measured in order to characterize and compare the performance characteristics, such as responsivity and detectivity in three configurations of micro-bolometers: (a) planar structure with a silicon–germanium intrinsic (a-Si_xGe_y:H) thermo-sensing film; (b) planar structure with a silicon–germanium–boron alloy (a-$Si_xGe_yB_z$:H) thermo-sensing film and (c) sandwich structure with an intrinsic (a-Si_xGe_y:H) thermo-sensing film. The samples studied demonstrated different cell resistance $R_c = 10^5$–$10^8\ \Omega$ and responsivities $R_I = 10^1$–10^{-3} A/W, while the values of detectivity D^* were quite similar $D^* = (4–7) \times 10^9$ cm Hz$^{1/2}$ W^{-1}.

PACS: 07.57.Kp

Keywords: Amorphous semiconductors; Germanium; Silicon; Sensors

1. Introduction

Surface micro-machining technology for thin films in conjunction with the silicon IC fabrication technology have allowed an important development on low cost and reliable night vision systems based on thermal detectors arrays. A micro-bolometer is a thermal detector used for large IR arrays. Even in the actuality there are available large micro-bolometer arrays [1–4], none of them can be considered to contain an optimum pixel.

In order to achieve high performance characteristics in a micro-bolometer, it should have a thermo-sensing film with a high value of the temperature coefficient of resistance (TCR), defined as $\alpha(T) = (1/R)|dR/dT| \approx E_a/kT^2$, where E_a is the activation energy of the thermo-sensing film; moderated resistivity, low noise, fast response time, and compatibility with standard silicon IC technology. Among the currently thermo-sensing materials used in micro-bolometers, some metals, vanadium oxide, and amorphous silicon [1–4] should be mentioned.

Those materials present good characteristics but also have some disadvantages. Metals are compatible with the standard IC fabrication technology, but have low E_a and consequently low TCR values. Vanadium oxide presents a high TCR but it is not a standard material in IC technology. Amorphous silicon (a-Si:H) has shown a high TCR value [3] and is fully compatible with the silicon technology, however possesses a very high resistance, which results in a mismatch with the input impedance of the CMOS read-out circuits. In our previous work [5] amorphous silicon–germanium films obtained by PECVD were employed in the fabrication of micro-bolometers, providing high activation energy ($E_a = 0.34$ eV) and improved, but still high resistivity.

In this work we report a comparative study of the performance characteristics of three configurations of un-cooled micro-bolometers based on amorphous silicon–germanium thin films: (a) planar structure with silicon–germanium a-Si_xGe_y:H thermo-sensing film. In this configuration the metal electrodes are placed under the thermo-sensing film

* Corresponding author. Tel.: +52 222 2663100; fax: +52 222 2470517. *E-mail address:* akosarev@inaoep.mx (A. Kosarev).

0022-3093/$ - see front matter
doi:10.1016/j.jnoncrysol.2007.09.116

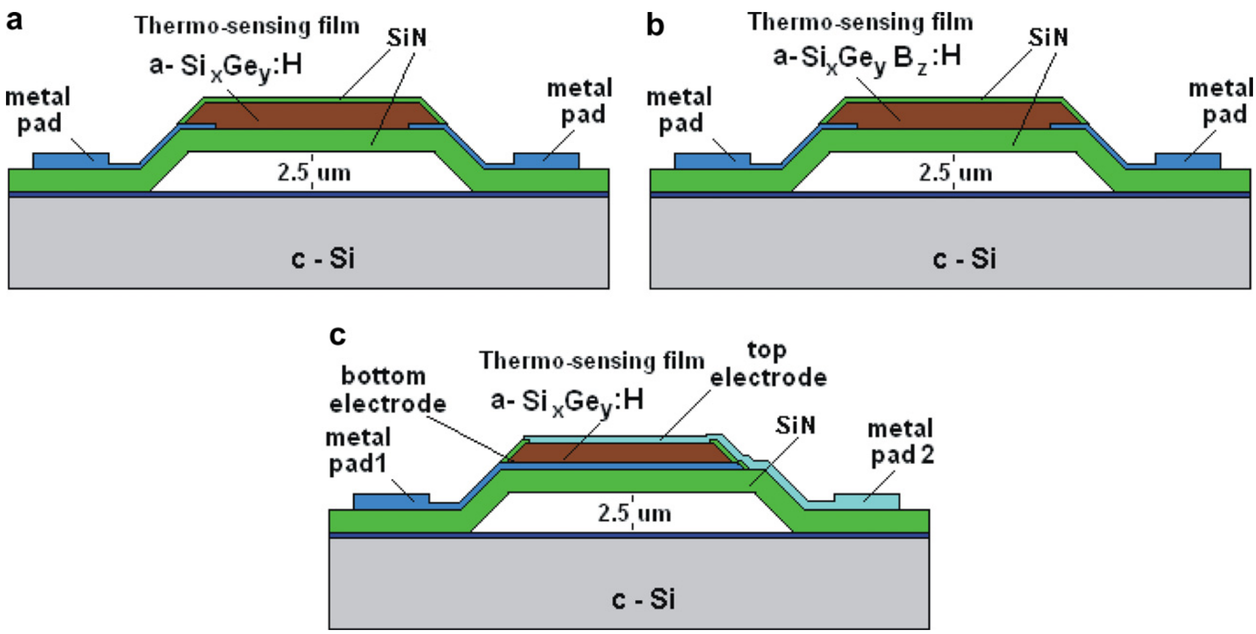

Fig. 1. Micro-bolometer structures: (a) planar with a-Si_xGe_y:H, (b) planar with a-$Si_xGe_yB_z$:H and (c) sandwich with a-Si_xGe_y:H.

(Fig. 1(a)); (b) planar structure with an a-$Si_xGe_yB_z$:H thermo-sensing film (Fig. 1(b)). The latter is a silicon–germanium–boron alloy rather than a boron doped film and (c) sandwich structure with a-Si_xGe_y:H thermo-sensing film, this configuration consists of metal electrodes which sandwich the thermo-sensing film (Fig. 1(c)).

2. Experimental

The fabrication process of the planar structure micro-bolometer with the a-Si_xGe_y:H thermo-sensing film is as follows. A 0.2 μm-thick SiO_2 layer was deposited by CVD on a c-Si wafer and a 2.5 μm-thick sacrificial aluminum layer was deposited by e-beam evaporation and patterned. A 0.8 μm-thick SiN film was deposited at low temperature (350 °C) by low frequency PE CVD over the aluminum sacrificial film. The SiN film is patterned by reactive ion etching (RIE) in order to form a SiN bridge. 0.2 μm-thick titanium contacts were deposited by e-beam evaporation over the SiN bridge. A 0.5 μm-thick thermo-sensing a-Si_xGe_y:H film was deposited over the Ti contacts by low frequency LF PECVD at a RF frequency $f = 110$ kHz, substrate temperature $T = 300$ °C, power $W = 350$ W, and pressure $P = 0.6$ Torr. The a-Si_xGe_y:H film was deposited from a $SiH_4 + GeH_4 + H_2$ mixture with gas flow rates: $Q_{SiH_4} = 25$ sccm, $Q_{GeH_4} = 25$ sccm, $Q_{H_2} = 1000$ sccm. This results in a Ge content in the solid phase of $Y = 0.88$, and a Si content in the solid phase of $X = 0.11$. The thermo-sensing film was covered with a 0.2 μm-thick absorbing SiN film deposited by PECVD and finally the aluminum sacrificial layer was removed with wet etching.

The planar structure micro-bolometer with the boron alloy (a-$Si_xGe_yB_z$:H) thermo-sensing film was fabricated as the previous one, with different thermo-sensing film deposition parameters. The boron alloy film was deposited from a $SiH_4 + GeH_4 + B_2H_6 + H_2$ mixture with the following gas flow rates: $Q_{SiH_4} = 50$ sccm, $Q_{GeH_4} = 50$ sccm, $Q_{B_2H_6} = 5$ sccm and $Q_{H_2} = 500$ sccm. This results in a Ge content in the solid phase of $Y = 0.67$, a Si content in the solid phase of $X =$ and B content in the solid phase of $Z = 0.26$. Those values were obtained by SIMS measurements.

The sandwich structure micro-bolometer with the a-Si_xGe_y:H film was fabricated in the same way as the planar micro-bolometer with some differences, due to the placement of metals as bottom and top electrodes. In this structure the electrodes sandwich the thermo-sensing film. The bottom Ti electrode is 0.2 μm-thick and is deposited before the thermo-sensing film. Then the a-Si_xGe_y:H film is deposited and it is covered with a top thin electrode (10 nm) forming a sandwich structure. The active area of the thermo-sensing layer in the three configurations studied is $A_b = 70 \times 66$ μm^2.

In order to compare the performance characteristics in the three micro-bolometer configurations, we performed the measurement of $I(U)$ characteristics in darkness and under IR illumination conditions. The source of IR light is a SiC globar source (model LSH-GB from Jobin Yvon), which provides intensity $I_0 = 5.3 \times 10^{-2}$ W/cm^2 in the range of $\lambda = 1$–20 μm. The samples were placed in a vacuum thermostat at pressure $P \approx 20$ mTorr, at room temperature and illuminated through a zinc selenide window (ZnSe). The window has a 70% transmission in the range of $\lambda = 0.6$–20 μm. The current was measured with an electrometer (‘Keithley’ – 6517-A) and the responsivity was calculated from the $I(U)$ measurements. Noise measurements in the micro-bolometers were performed with a lock-in amplifier (‘Stanford Research Systems’ – SR530).

The noise of the system and the total noise (system + cell noise) were measured separately, and a subtraction of the system noise allowed us to obtain the noise of the device. The detectivity was calculated from the $I(U)$ characteristics and noise measurements.

3. Results

We measured the thermal dependence of conductivity in the thermo-sensing films used in the micro-bolometers in a temperature range of $T = 300$–400 K. The activation

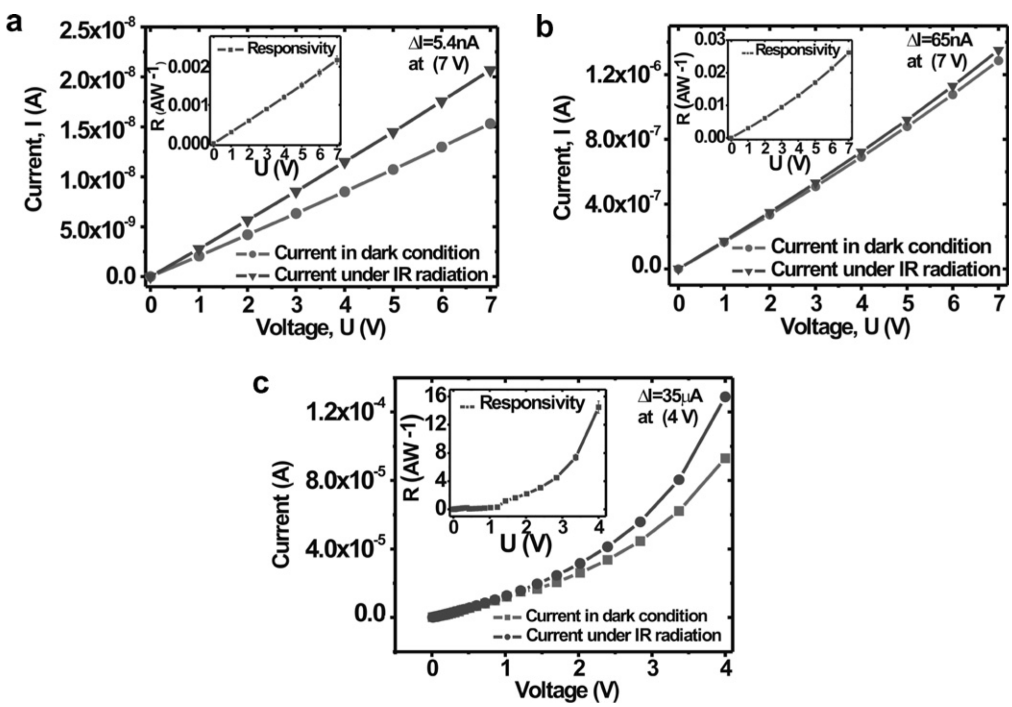

Fig. 2. $I(U)$ characteristics of micro-bolometer: (a) planar with a-Si_xGe_y:H, (b) planar with a-$Si_xGe_yB_z$:H and (c) sandwich with a-Si_xGe_y:H.

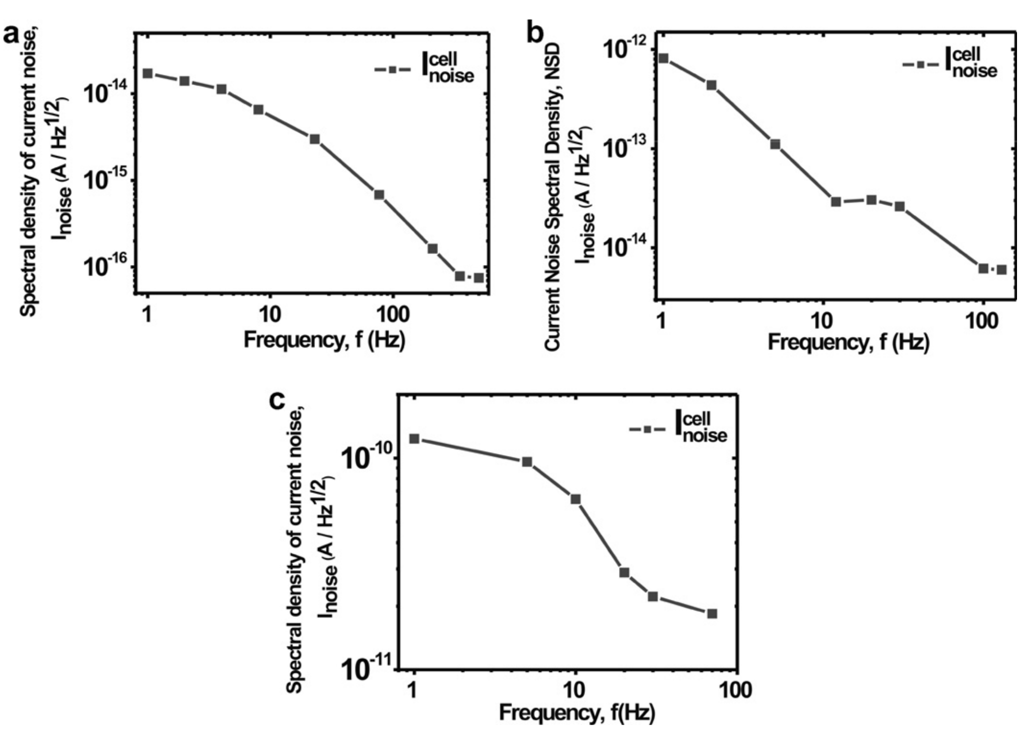

Fig. 3. Spectral density of current noise, I_{noise} as a function of frequency of the micro-bolometers: (a) planar with a-Si_xGe_y:H, (b) planar with a-$Si_xGe_yB_z$:H and (c) sandwich with a-Si_xGe_y:H.

Table 1
Comparison of the characteristics of micro-bolometers

Thermo-sensing layer	E_a (eV)	TCR, α (K^{-1})	Pixel area, A_b (μm^2)	Pixel resistance, R_b (Ω)	Voltage responsivity, R_U ($V W^{-1}$)	Current responsivity R_I (A/W)	Spectral response (μm)	Detectivity, D[a] (cm $Hz^{1/2} W^{-1}$)	Reference
a-Si:H,B	0.22	0.028	48 × 48	3×10^7	10^6	–	5 – 14	–	[3]
a-Si_xGe_y:H	0.34	0.043	70 × 66	1×10^5	2×10^5[a]	0.3–14	2 – 14	$4 \times 10^9 \pm 1 \times 10^9$	Sandwich structure
a-$Si_xGe_yB_z$:H	0.21	0.027	70 × 66	1×10^6	2.8×10^5[a]	2.6×10^{-2}	2 – 14	$5.9 \times 10^9 \pm 3.6 \times 10^8$	Planar structure
a-Si_xGe_y:H	0.34	0.043	70 × 66	5×10^8	7.2×10^5[a]	2×10^{-3}	2 – 14	$7 \times 10^9 \pm 3.3 \times 10^8$	Planar structure

[a] Voltage responsivity R_U, was calculated from the current responsivity R_I.

energy of the a-Si_xGe_y:H film used in planar and sandwich micro-bolometers was measured in a test structure, it is $E_a = 0.34$ eV providing a TCR $\alpha = 0.043\ K^{-1}$ and a dark conductivity at room temperature $\sigma_{RT} = 6 \times 10^{-5}\ \Omega^{-1}\ cm^{-1}$. While the activation energy of the a-$Si_xGe_yB_z$:H film used in planar micro-bolometers measured in a test structure is $E_a = 0.21$ eV providing a TCR $\alpha = 0.027\ K^{-1}$ and a dark conductivity at room temperature $\sigma_{RT} = 1.3 \times 10^{-2}\ \Omega^{-1}\ cm^{-1}$.

Fig. 2 shows the current–voltage $I(U)$ characteristics in darkness and under IR illumination for the configurations studied: planar with a-Si_xGe_y:H thermo-sensing film (2a), planar with a-$Si_xGe_yB_z$:H thermo-sensing film (2b) and sandwich with a-Si_xGe_y:H thermo-sensing film (2c). In those figures we can see the increment in current due to IR illumination, $\Delta I = I_{IR} - I_{Dark}$, where I_{IR} is the current under IR radiation and I_{Dark} is the current in darkness. The planar configuration with a-Si_xGe_y:H has a $\Delta I = 5.4$ nA (at bias voltage $U = 7$ V); the planar configuration with a-$Si_xGe_yB_z$:H has a $\Delta I = 65$ nA (at bias voltage $U = 7$ V) and the sandwich configuration with a-Si_xGe_y:H has a $\Delta I = 35\ \mu$A (at bias voltage $U = 4$ V).

The insert in Fig. 2 shows the current responsivity for: planar micro-bolometer with a-Si_xGe_y:H film (insert of 2a), planar micro-bolometer with a-$Si_xGe_yB_z$:H film (insert of 2b) and sandwich with a-Si_xGe_y:H film (insert of 2c). The current responsivity R_I, is defined as $R_I = \Delta I / P_{inc}$, where $P_{inc} = I_0 \times A_b$, I_0 is the incident IR intensity and A_b is the bolometer area. The planar micro-bolometer with a-Si_xGe_y:H film has a $R_I = 2 \times 10^{-3}$ A/W (at $U = 7$ V); the planar micro-bolometer with a-$Si_xGe_yB_z$:H film has a $R_I = 3 \times 10^{-2}$ A/W (at $U = 7$ V) and the sandwich micro-bolometer with a-Si_xGe_y:H film has a $R_I = 14$ A/W (at $U = 4$ V).

The current noise spectral density (NSD), $I_{cell\ noise}(f)$, is shown in Fig. 3, where $(I_{cell\ noise}(f))^2 = (I_{system + cell\ noise}(f))^2 - (I_{system\ noise}(f))^2$: $I_{cell + system\ noise}(f)$ is the NSD measured at the micro-bolometer with the measuring system and the $I_{system\ noise}(f)$ is the NSD measured in the system without the micro-bolometer. The planar structure with a-Si_xGe_y:H film presents $I_{cell\ noise}(f) \approx 10^{-16}\ A\ Hz^{-1/2}$, the planar structure with a-$Si_xGe_yB_z$:H film presents $I_{cell\ noise}(f) \approx 10^{-14}\ A\ Hz^{-1/2}$, while the sandwich structure with a-Si_xGe_y:H presents $I_{cell\ noise}(f) \approx 10^{-11}\ A\ Hz^{-1/2}$.

4. Discussion

From $I(U)$ measurements we observed a reduction in cell resistance from $R_{cell} \approx 10^8\ \Omega$ in the planar structure with the a-Si_xGe_y:H film, to $R_{cell} \approx 1 \times 10^6\ \Omega$ in the planar structure with the a-$Si_xGe_yB_z$:H film and to $R_{cell} \approx 1 \times 10^5\ \Omega$ for the sandwich structure with the a-Si_xGe_y:H film.

The sandwich structure micro-bolometer with the a-Si_xGe_y:H film presents the largest responsivity, while the planar structure micro-bolometer with the a-Si_xGe_y:H film presents the smallest responsivity; however, the planar structure with a-Si_xGe_y:H film presents the lowest $I_{cell\ noise}$, while the sandwich structure with a-Si_xGe_y:H presents the largest $I_{cell\ noise}$.

From the responsivity and noise measurements, we calculated the detectivity values D^* in the three structures. For the planar structure with the a-Si_xGe_y:H film we obtained $D^* = 7 \times 10^9 \pm 3.3 \times 10^8\ cm\ Hz^{1/2}\ W^{-1}$, for the planar structure with the a-$Si_xGe_yB_z$:H film it is $D^* = 5.9 \times 10^9 \pm 3.6 \times 10^8\ cm\ Hz^{1/2}\ W^{-1}$ and for the sandwich structure micro-bolometer with the a-Si_xGe_y:H film it is $D^* = 4 \times 10^9 \pm 1 \times 10^9\ cm\ Hz^{1/2}\ W^{-1}$ The performance characteristics of the three structures studied are listed in Table 1 and are compared with data reported in the literature.

5. Conclusions

The largest current responsivity was found in the sandwich structure with the intrinsic a-Si_xGe_y:H film, $R_I = 14$ A/W; in the planar structure with the boron alloy a-$Si_xGe_yB_z$:H film it was $R_I = 3 \times 10^{-2}$ A/W and the smallest value was in the planar configuration with the intrinsic a-Si_xGe_y:H film, $R_I = 2 \times 10^{-3}$. However, the sandwich structure presents the larger NSD value $I_{cell\ noise}(f) \approx 10^{-11}\ A\ Hz^{-1/2}$, in the planar structure with the boron alloy it is equal to $I_{cell\ noise}(f) \approx 10^{-14}\ A\ Hz^{-1/2}$ and in the planar structure with the intrinsic film it is equal to $I_{cell\ noise}(f) \approx 10^{-16}\ A\ Hz^{-1/2}$. Therefore despite of differences in responsivities and NSD values, the detectivity values are quite similar in the devices studied, $D^* = (4-7) \times 10^9\,\mathrm{cm\,Hz^{1/2}\,W^{-1}}$.

Acknowledgments

The authors acknowledge the support of this research by CONACyT project No. 48454 and would like to thank Dr Y. Kudriavtsev from CINVESTAV, Mexico for SIMS characterization of the samples. M. Moreno acknowledges CONACyT for support granted through scholarship # 166011.

References

[1] J.L. Tissot, Opto-electron. Rev. 12 (1) (2004) 105.
[2] Eric Mottin, Astrid Bain, Jean-Luc Martin, Jean-Louis Ouvrier-Buffet, Sylvette Bisotto, Jean-Jacques Yon, Jean-Luc Tissot, in: XXVIII SPIE Proc., vol. 4820, 2003, p. 200.
[3] A.J. Syllaios, T.R. Schimert, R.W. Gooch, W.L. McCardel, B.A. Ritchey, J.H. Tregilgas, Mater. Res. Soc. Symp. Proc. 609 (2000) A14.4.1.
[4] J.J. Yon, A. Astier, S. Bisotto, G. Chamingis, A. Durand, J.L. Martin, E. Mottin, J.L. Ouvrier-Buffet, J.L. Tissot, in: XXXI SPIE Proc., vol. 5783, 2005, p. 432.
[5] R. Ambrosio, A. Torres, A. Kosarev, A. Illinski, C. Zúñiga, A.S. Abramov, J. Non-Cryst. Solids 338–340 (2004) 91.